Cogn Neurodyn (2016) 10:113–120
DOI 10.1007/s11571-015-9359-8

RESEARCH ARTICLE

Default network connectivity decodes brain states with simulated microgravity

Ling-Li Zeng[1] · Yang Liao[2] · Zongtan Zhou[1] · Hui Shen[1] · Yadong Liu[1] · Xufeng Liu[2] · Dewen Hu[1]

Received: 21 August 2015 / Revised: 25 September 2015 / Accepted: 8 October 2015 / Published online: 14 October 2015

Abstract With great progress of space navigation technology, it becomes possible to travel beyond Earth's gravity. So far, it remains unclear whether the human brain can function normally within an environment of microgravity and confinement. Particularly, it is a challenge to figure out some neuroimaging-based markers for rapid screening diagnosis of disrupted brain function in microgravity environment. In this study, a 7-day −6° head down tilt bed rest experiment was used to simulate the microgravity, and twenty healthy male participants underwent resting-state functional magnetic resonance imaging scans at baseline and after the simulated microgravity experiment. We used a multivariate pattern analysis approach to distinguish the brain states with simulated microgravity from normal gravity based on the functional connectivity within the default network, resulting in an accuracy of no less than 85 % via cross-validation. Moreover, most discriminative functional connections were mainly located between the limbic system and cortical areas and were enhanced after simulated microgravity, implying a self-adaption or compensatory enhancement to fulfill the need of complex demand in spatial navigation and motor control functions in microgravity environment. Overall, the findings suggest that the brain states in microgravity are likely different from those in normal gravity and that brain connectome could act as a biomarker to indicate the brain state in microgravity.

Keywords Microgravity · Functional magnetic resonance imaging · Connectome · Multivariate pattern analysis · Default network

Introduction

With great progress of space navigation technology, it becomes possible to travel beyond Earth's gravity. Maintaining astronauts' performance at a good level is a hot topic among space medical and psychological researchers. It is known that astronauts' performance would be impaired due to potential harmful factors in the outer space such as radiation, noise, changed circadian rhythm, weightlessness and so on (Eddy et al. 1998). Among these factors, weightlessness exhibits the most significant difference between space environment and earth environment, thus the astronauts' performance degradation caused by weightlessness has become a common focus.

A number of previous studies reported various performance degradations happened to astronauts in weightlessness and attempted to seek the mechanism (Mallis and De Roshia 2005; Manzey et al. 2000; Moore et al. 2010; Pavy-Le Traon et al. 2007; Vaitl et al. 1996; Zhao et al. 2011). Some researchers lay their sight on the common known redistribution of body fluid effect induced by gravity change (Grigoriev and Egorov 1992; Liao et al. 2012;

Ling-Li Zeng and Yang Liao have contributed equally to this work.

✉ Dewen Hu
dwhu@nudt.edu.cn

Xufeng Liu
lllfmmu@fmmu.edu.cn

[1] College of Mechatronics and Automation, National University of Defense Technology, Changsha 410073, Hunan, People's Republic of China

[2] Department of Psychology, Fourth Military Medical University, Xi'an 710032, Shaanxi, People's Republic of China

Messerotti Benvenuti et al. 2011; Vaitl et al. 1996). Especially, the cephalad fluid shift may alter the hemodynamics of the brain, including increase in cerebral blood flow (CBF), intracranial pressure, and oxygenated hemoglobin (Kawai et al. 2003), all of which may influence the function of the human brain. Liao et al. (2013) tentatively used resting-state functional magnetic resonance imaging (fMRI) to investigate brain activity change after 3-day head down tilt (HDT) bed rest and observed decreased local activity in thalamus and declined regional homogeneity in left inferior parietal lobule which may attribute to reduced motor control abilities and declined abilities of mental transformation. Recently, Zhou et al. (2014) carried out a groundbreaking research to discuss the effects of long-term microgravity on the functional architecture of the brain. In this 45-day HDT bed rest study, a functional network anchored in the anterior insula and middle cingulate cortex was found to be influenced by simulated microgravity. The authors suggested that these functional anomalies may reflect variation in cognitive function, autonomic neural function and central neural activity (Zhou et al. 2014). In a recent study, Liao et al. (2015) figured out the time trend of brain activity change in a 7-day HDT period. These imaging studies further our insight in performance decline happened to astronauts under microgravity, describing the cumulative effects of microgravity in different time span. The aforementioned studies came out to a single truth that the brain activity is changing with microgravity and could be quantifiably measured by resting-state fMRI. Then a new challenge is coming, could we figure out some suitable neuroimaging-based markers to effectively distinguish the brain states in microgravity and normal gravity? This may contribute to the rapid screening diagnosis of disrupted brain function in microgravity environment.

The default network (DN) is demonstrated to support autobiographical memory retrieval, prospection, monitoring, and other internal mentation (Buckner et al. 2008). The alterations associated with DN play promising biomarkers in neuropsychiatric disorders (Garrity et al. 2007; Zeng et al. 2012), so we speculate that the default connectivity can be used as an indicator of brain states with simulated microgravity. In the current study, twenty healthy male subjects underwent a 7-day-6° HDT bed rest experiment, which is generally accepted to simulate the microgravity effect of body fluid redistribution toward the head (Baisch et al. 1992). So we can study the effects of microgravity on brain function on the Earth. The participants underwent resting-state fMRI scanning at baseline and after 7-day HDT simulated microgravity experiment. We tested whether the default functional connectivity could distinguish brain states with simulated microgravity from baseline (normal gravity).

Materials and methods

Participants

Twenty healthy male participants were recruited for the present study. Their mean age was 24 years with a range from 20 to 32 years and their mean weight was 62.5 kg with a range from 51 to 82 kg. All participants were right-handed Chinese speakers, as measured by the Handedness Questionnaire (Annett 1970). The participants reported no history of neurological injury, genetic mental disorders or substance abuse. With a high-resolution T1- and T2-weighted MRI examination, no participant was observed to have significant pathological changes in their brains. The study was approved by the Ethical Committee of the Fourth Military Medical University and all participants provided their written informed consent before the experiment.

Design

The whole experiment was divided into three periods: prior bed rest period (HDT0, baseline), bed rest period (HDT1–HDT7) and post bed rest period (7 days after bed rest, HDT14). Resting-state fMRI scans were taken at 19:00 every experiment day, which means that every participant received MRI scans for 9 times in total. During the HDT bed rest, adequate water and food were supplied, but the participants' heads were prevented from moving from the bed to keep the redistribution of the individual's body fluid toward the head. The experimental room was air-conditioned, and the temperature was maintained around 22 °C. All of the testers are well educated with medical knowledge and skills, thus they could provide nursing care to the participants. Additionally, the participants were pared and they were allowed to communicate with each other or take some recreational activities (such as reading, watching TV or movies, surfing on the internet and so on) in their leisure time. In this study, only the data of the HDT0 and HDT7 were used.

Image acquisition and preprocessing

All data were collected by an experienced radiologist on a 3.0-T Philips Achieva MRI scanner with an 8-channel phased-array head coil in the Radiology Department of the P.L.A. 303 Hospital. Images were acquired using a gradient-echo echo-planar pulse sequence sensitive to blood oxygenation level-dependent (BOLD) contrast [repetition time (TR)/echo time (TE) = 2000/35 ms, flip angle (FA) = 90°, matrix = 96 × 93, field of view (FOV) = 230, thickness = 4 mm, slices = 36 with no gap]. The resting-state fMRI runs lasted 6 min and 40 s, resulting in 200 fMRI time

points. Each session had two resting-state fMRI runs. Structural data used a high-resolution multi-echo T1-weighted magnetization-prepared gradient-echo image (TR/TE = 7.6/3.5 ms, flip angle = 8°, FOV = 250, matrix = 512 × 512, slice thickness = 0.6 mm with no gap, and 301 slices). Subjects were instructed to stay awake, keep their eyes closed, and minimize head movement; no other task instruction was provided.

Data were preprocessed using previously described procedures (Zeng et al. 2014) with the statistical parametric mapping software package (SPM8, Welcome Department of Cognitive Neurology, Institute of Neurology, London, UK, http://www.fil.ion.ucl.ac.uk/spm). The first five volumes of each run were discarded to allow for T1-equilibration effects, Then the slicing timing, motion correction, normalization with an EPI template in the Montreal Neurological Institute (MNI) atlas space (3-mm isotropic voxels), spatial smoothing using a 6-mm full-width half-maximum (FWHM) Gaussian kernel, linear detrend and band-pass temporal filtering (0.01–0.08 Hz) were performed. Finally, the nuisance variables including the six parameters obtained by rigid body head motion correction, global signal, ventricular and white matter signals, and the first temporal derivatives of all the above were regressed out.

Default functional connectivity measure

A collection of 19 functional regions of interest (ROIs) was used as default seed regions to define default connectivity (Shirer et al. 2012), including 9 dorsal and 10 ventral default regions (Table 1). Regional time courses were obtained for each session by averaging the BOLD time courses over all voxels in each of the 19 default ROIs. Connectivity has been widely used in the analysis of temporal interactions between cortical regions (Dimitriadis et al. 2015; Seth 2008; Wilmer et al. 2010). We evaluated functional connectivity between each pair of ROIs using Pearson correlation coefficient, and all correlations were then translated to z-values by applying Fisher r-to-z transformation. Thus, we obtained a default connectivity matrix captured by a 19 × 19 symmetric correlation matrix for each session. Finally, the default connectivity matrix for each session was converted to a feature vector containing 171 unique region-to-region connections (19 × 18/2).

Multivariate pattern classification

First, two-tailed paired t tests were used during training to identify the features that are most distinct between baseline and simulated microgravity. Considering the feature number as a parameter, the optimal number of features with the lowest p values would be obtained when the classifier achieved peak accuracy. Then support vector machines (SVMs) with linear and polynomial (nonlinear) kernel functions combined with locally linear embedding (LLE) were trained and tested based on the features defined as region-to-region connections (Roweis and Saul 2000; Vapnik 1995), respectively. All classification analyses were implemented in MATLAB using the SVM toolbox developed by S. Gunn (http://www.isis.ecs.soton.ac.uk/resources/svminfo/), and the slack parameter C in the SVMs was set as the default value ($C = 1$). The algorithms were reported with the best parameter settings (The manifold dimensionality in LLE was 32, and the number of nearest neighbors in LLE for linear and polynomial SVMs were 4 and 5, respectively).

Due to the limited number of samples, we used a leave-one-subject-out cross-validation strategy to estimate the generalization ability of the classification algorithms, i.e., the connectivity feature vectors at baseline and with simulated microgravity of a given subject were used as testing data (one subject, two sessions) and the remainder were used as training data (18 subjects, 36 sessions). The performance of a classifier can be quantified using the generalization rate (GR), sensitivity (SS), and specificity (SC) based on the results of cross-validation (Fawcett 2006). Note that the SS represents the proportion of samples correctly predicted with simulated microgravity, while the SC represents the proportion of samples correctly predicted at baseline. The overall proportion of samples correctly predicted is evaluated by the GR. In addition, a receiver operating characteristic (ROC) curve was generated to evaluate the classification performance (Fawcett 2006). A classifier better than random should yield an area under the curve (AUC) greater than 0.5. The flowchart of the classification can be seen in Fig. 1.

To illuminate which default connections most contributed to the classification, consensus connections were defined as the connectivity features appearing in the final feature set of each cross-validation iteration (Dosenbach et al. 2010). To enhance the reliability of the discriminative default connections, we defined the most discriminative default connections as the consensus connections with p value less than 0.05 in paired t tests.

Results

Classification results

The classification results via leave-one-subject-out cross-validation can be seen in Table 2 and Fig. 2. The polynomial SVM classifiers with LLE achieved a peak accuracy of 87.5 % (SS = 90 %, SC = 85 %, AUC = 0.883). Even using linear kernel function, the SVM classifiers could

Table 1 Functional regions of interest (ROIs) within the default network

ROI name	Side	Brodmann area	MNI coordinates (x, y, z)	Subsystem
Medial prefrontal cortex		9, 10, 24, 32, 11	−3, 49, 14	Dorsal default
Inferior parietal lobule	L	39	−48, −68, 35	Dorsal default
Superior frontal gyrus	R	9	19, 38, 47	Dorsal default
Posterior cingulate cortex		23, 30	1, −53, 28	Dorsal default
Midcingulate cortex		23	2, −15, 36	Dorsal default
Right angular cortex	R	39	50, −64, 32	Dorsal default
Thalamus			−1, −8, 4	Dorsal default
Hippocampus	L	20, 36, 30	−24, −29, −13	Dorsal default
Hippocampus	R	20, 36, 30	27, −23, −17	Dorsal default
Retrosplenial cortex	L	29, 30, 23	−12, −58, 15	Ventral default
Middle frontal gyrus	L	8, 6	−24, 12, 55	Ventral default
Parahippocampal gyrus	L	37, 20	−28, −37, −15	Ventral default
Middle occipital gyrus	L	19, 39	−36, −81, 32	Ventral default
Retrosplenial cortex	R	30, 23	13, −53, 14	Ventral default
Precuneus		7, 5	1, −57, 54	Ventral default
Superior frontal gyrus	R	9, 8	26, 26, 45	Ventral default
Parahippocampal gyrus	R	37, 30	28, −33, −19	Ventral default
Inferior parietal lobule	R	39, 19	43, −74, 32	Ventral default
Cerebellar lobule 9	R		15, −46, −53	Ventral default

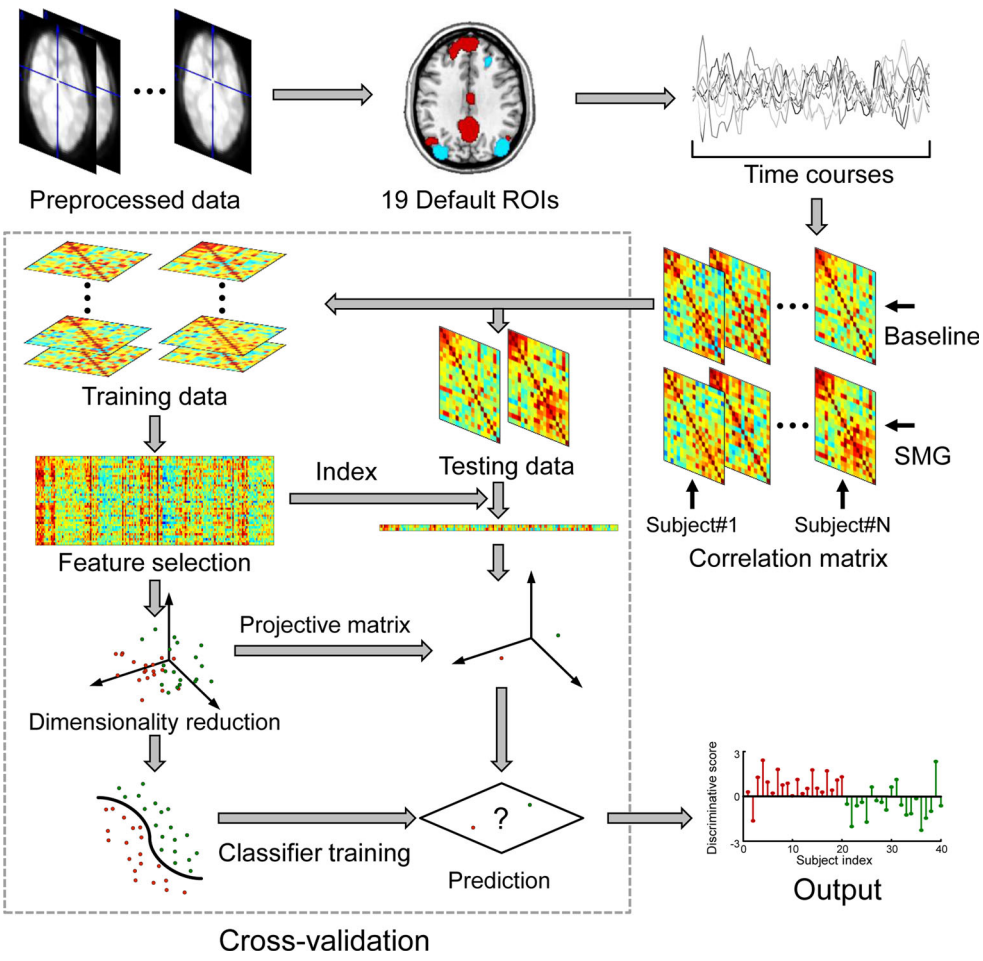

Fig. 1 The flowchart of the classification with a leave-one-subject-out cross-validation strategy. *ROI* Region of interest, *SMG* Simulated microgravity

Table 2 Classification results with different algorithms

Algorithm	Training dataset (%)	SS (%)	SC (%)	GR (%)	AUC
SVM (linear)	99.5	70	70	70	0.600
SVM (polynomial)	99.9	70	70	70	0.625
LLE + SVM (linear)	99.9	75	95	85	0.820
LLE + SVM (polynomial)	100	90	85	87.5	0.883

AUC Area under the receiver operating characteristic (ROC) curve, *GR* Generalization rate, *LLE* Local linear embedding, *SC* Specificity, *SS* Sensitivity, *SVM* Support vector machine

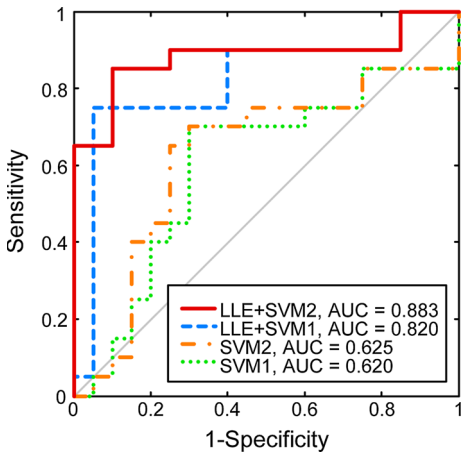

Fig. 2 The ROC curves of the classifications. It is noted that the polynomial SVM classifiers with LLE achieved a peak accuracy of 87.5 % (*Red line*, SS = 90 %, SC = 85 %, AUC = 0.883). AUC, area under the receiver operating characteristic (ROC) curve; *LLE* Local linear embedding; SVM1/2, support vector machine with linear/polynomial kernel functions. (Color figure online)

differentiate the brain connectivity states after simulated microgravity from baseline with an accuracy of 85 % (SS = 75 %, SC = 90 %, AUC = 0.820). However, both of the two SVMs (linear and polynomial) achieved accuracies of 70 % without nonlinear dimensionality reduction (LLE).

To exclude potential confounding effect of scanning interval, we leaved two subjects out in the cross validation, and the one's HDT0 scanning date is later than the other's HDT7 scanning date. Then we used the remaining subjects' data as training data and these two sessions as testing data, discarding two other sessions of the two subjects. In this regard, the date of HDT0 is latter than that of HDT7 in the testing sample, eliminating the scanning interval (in the original analyses, the date of HDT0 is earlier than that of HDT7 in the testing sample). The classification results revealed that both the linear and polynomial SVM classifiers with LLE achieved a peak accuracy of 83.3 % (SS = 88.9 %, SC = 78.8 %, AUC = 0.787), suggesting the confounding effect of scanning interval is limited in the current study.

Most discriminative functional connectivity

The most discriminative default connections were mainly located between the limbic system and cortical areas, as shown in Fig. 3. The left retrosplenial cortex (RSC) exhibited enhanced functional connectivity with the left inferior parietal lobule (IPL, $p = 0.023$), midcingulate cortex ($p = 0.017$) and left hippocampus ($p = 0.012$), and the thalamus showed increased connectivity with the left IPL ($p = 0.016$) and medial prefrontal cortex (mPFC, $p = 0.042$) but decreased connectivity with the right IPL ($p = 0.039$), and the right superior frontal gyrus exhibited increased connectivity with the left IPL ($p = 0.026$) and middle occipital gyrus ($p = 0.044$). In addition, the left middle frontal gyrus exhibited enhanced connectivity with the left parahippocampal gyrus ($p = 0.028$) and midcingulate cortex ($p = 0.015$).

Discussion

In this study, we used a multivariate pattern analysis approach combining SVM with LLE to distinguish the brain states with simulated microgravity from baseline based on the functional connectivity within the default network, resulting in an accuracy of no less than 85 % via leave-one-subject-out cross-validation. The results suggest that the brain states with simulated microgravity are likely different from that at baseline and that brain connectome could act as a biomarker to indicate the brain state with microgravity.

In this study, it was observed that the SVM classifiers with both linear and polynomial kernel functions could differentiate the brain connectivity states after simulated microgravity from baseline with an accuracy of no less than 85 %, implying the independence of classification performance from the SVM kernel functions to some extent. However, both of the two SVMs (linear and polynomial) achieved accuracies of 70 % without nonlinear dimensionality reduction such as the LLE, suggesting that as a nonlinear manifold learning technique, the LLE is capable of obtaining a low dimensional embedding of the data while preserving the intrinsic data structures and helps

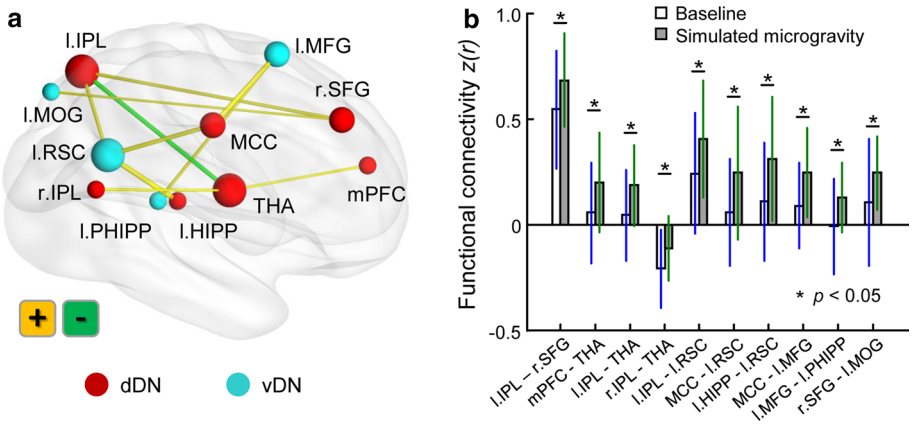

Fig. 3 The most discriminative default functional connectivity in decoding brain states with simulated microgravity. It is noted that most connections were located between the limbic system and cortical areas and were enhanced after simulated microgravity relative to the baseline. *HIPP* Hippocampus, *IPL* Inferior parietal lobule, *MCC* Midcingulate cortex, *MFG* Middle frontal gyrus, *MOG* Middle occipital gyrus, *PHIPP* Parahippocampal gyrus, *RSC* Retrosplenial cortex, *SFG* Superior frontal gyrus, *THA* thalamus, *mPFC* Medial prefrontal cortex, *dDN/vDN* dorsal/ventral default network, *l/r Left/right*

to enhance the classification performance. Whatsoever, these results suggest that the brain states after simulated microgravity are indeed likely to be different from baseline and that the default functional connectivity could provide potential evidence for the brain state evaluation within an environment of microgravity.

The DN is believed to support internal mentation (Buckner et al. 2008), and the default-associated abnormalities have been demonstrated in many neuropsychiatric disorders (Garrity et al. 2007; Zeng et al. 2012). In the current study, the default functional connectivity could separate the brain states with simulated microgravity from baseline, suggesting that the microgravity could induce brain connectivity changes within the DN and that the default functional connectivity could be used as an indicator of brain states with microgravity.

In the present study, RSC showed enhanced connectivity with IPL, midcingulate cortex, and hippocampus in HDT period. Recent human functional imaging studies suggest that RSC is one of brain areas underlying spatial navigation (Bar 2004; Epstein 2008; Epstein et al. 2007; Henderson et al. 2007, 2008; Spiers and Maguire 2006; Spreng et al. 2009). Particularly, cooperating with hippocampus, RSC plays an important role in representing the shape of the environment and detecting the geometric relationships, which make it possible to use landmarks to navigate or orient in both novel and familiar environments (Aggleton et al. 2009; Aguirre and D'Esposito 1999; Kosaki et al. 2014; Maguire 2001; Pearce et al. 2004). Additionally, lesion studies have indicated that RSC is engaged in translating and changing spatial frames of reference from translating egocentric intraparietal into allocentric hippocampal multisensory representations of self-location (Burgess et al. 2001; Byrne et al. 2007; Vann and Aggleton 2002, 2004; Vann et al. 2009). In microgravity environment, human's body is always in inversion or tilted position, egocentric reference frame used on earth is no longer suitable for spatial navigation, an allocentric reference frame is in need. Actually, astronauts do use equipment in the cab as land markers during spaceflight. In this regard, the enhanced connectivity between RSC and hippocampus during HDT period in the present study may reflect a self-adaption process in spatial navigation function corresponding to environment change in microgravity. The thalamus was found to alter functional connectivity with mPFC and IPL in simulated microgravity. As a consensus, thalamus serves as an important center of information integration in brain. The thalamus has extensive connections with frontal regions and basal ganglia structure in anatomy and it modulate behaviors via several different pathways in function (Haber and Calzavara 2009). Additionally, both mPFC and IPL have been proved to engaged in motor control in previous structural and functional imaging studies (Alexander and Brown 2011; Andersen 2011; Borra et al. 2012; Desmurget and Sirigu 2012). Thus the altered connectivity between thalamus and the other two brain areas after HDT may partly account for motor function degeneration happened to astronauts during spaceflight, consistent with our previous studies (Liao et al. 2012).

Superior frontal gyrus and IPL have been testified to work together as part of parietal-frontal pathway which subserve spatial awareness in humans, participating the integration of auditory and visual inputs of spatial information (Bushara et al. 1999; de Schotten et al. 2005). In contrast, Middle occipital gyrus was only found to be sensitive to nonvisual inputs of spatial information (Renier et al. 2010). As visuospatial processing is more complex in

microgravity than on earth, the proper processing of non-visual inputs of spatial information may ease the dilemma in some extent. Comprehensively, the hyperactivity between superior frontal gyrus and those parietal and occipital areas after HDT may reflect the enhancement of auditory-spatial processing, which may serve as a supplement of visual orientation in microgravity environment. Due to the lack of data of auditory-spatial task in the present study, this assumption is still need to be clarified.

Middle frontal gyrus has been proved to be activated when humans represent spatial locations in short-term memory (Leung et al. 2002; Lockhart et al. 2015). Parahippocampal gyrus also plays an important role in spatial information progress, such as processing of the spatial location of objects, processing environmental landmarks and scene and spatial navigation (Aguirre et al. 1996; Owen et al. 1996). The enhanced functional connectivity between middle frontal gyrus and parahippocampal gyrus during HDT period may also reflect a self-adaption or compensatory enhancement process to fulfill the need of complex demand in spatial navigation function during spaceflight. Recent neuroimaging studies suggest that midcingulate cortex has a key role for cognitive aspects of movement generation, i.e., intentional motor control (Hoffstaedter et al. 2014). Increased connectivity between midcingulate cortex and middle frontal gyrus were found during HDT period, perhaps serving as a compensatory process to remission the problem of sensorimotor coordination in microgravity.

There are several limitations in the study. First, a control study should be done to exclude the potential confounding effect of the scanning interval, though we did a control analysis in the current study. Second, some specific neuropsychological tests should be designed and done to test whether there are relevant fine cognitive impairments after simulated microgravity experiment. Finally, the link between the default connectivity changes and cognitive behavioral performance needs to be explored in the future.

Funding This work was supported by the National Science Foundation of China (61503397, 61420106001, 91420302, 61375111, and 81272174) and National Basic Research Program of China (2013CB329401).

Compliance with ethical standards

Conflict of interest The authors declare that they have no conflict of interest.

References

Aggleton JP, Poirier GL, Aggleton HS, Vann SD, Pearce JM (2009) Lesions of the fornix and anterior thalamic nuclei dissociate different aspects of hippocampal-dependent spatial learning: implications for the neural basis of scene learning. Behav Neurosci 123:504–519

Aguirre GK, D'Esposito M (1999) Topographical disorientation: a synthesis and taxonomy. Brain 122:1613–1628

Aguirre GK, Detre JA, Alsop DC, D'Esposito M (1996) The parahippocampus subserves topographical learning in man. Cereb Cortex 6:823–829

Alexander WH, Brown JW (2011) Medial prefrontal cortex as an action-outcome predictor. Nat Neurosci 14:1338–1344

Andersen RA (2011) Inferior parietal lobule function in spatial perception and visuomotor integration. Compr Physiol. doi:10.1002/cphy.cp010512

Annett M (1970) A classification of hand preference by association analysis. Br J Psychol 61:303–321

Baisch F, Beck L, Karemaker J, Arbeille P, Gaffney F (1992) Head-down tilt bedrest HDT'88-an international collaborative effort in integrated systems physiology. Acta Physiol Scand 144:1–12

Bar M (2004) Visual objects in context. Nat Rev Neurosci 5:617–629

Borra E, Gerbella M, Rozzi S, Tonelli S, Luppino G (2012) Projections to the superior colliculus from inferior parietal, ventral premotor, and ventrolateral prefrontal areas involved in controlling goal-directed hand actions in the macaque. Cereb Cortex 24:1054–1065

Buckner RL, Andrews-Hanna JR, Schacter DL (2008) The brain's default network: anatomy, function, and relevance to disease. Ann NY Acad Sci 1124:1–38

Burgess N, Becker S, King JA, O'Keefe J (2001) Memory for events and their spatial context: models and experiments. Philos Trans R Soc Lond B Biol Sci 356:1493–1503

Bushara KO, Weeks RA, Ishii K, Catalan M-J, Tian B, Rauschecker JP, Hallett M (1999) Modality-specific frontal and parietal areas for auditory and visual spatial localization in humans. Nat Neurosci 2:759–766

Byrne P, Becker S, Burgess N (2007) Remembering the past and imagining the future: a neural model of spatial memory and imagery. Psychol Rev 114:340–375

de Schotten MT, Urbanski M, Duffau H, Volle E, Lévy R, Dubois B, Bartolomeo P (2005) Direct evidence for a parietal-frontal pathway subserving spatial awareness in humans. Science 309:2226–2228

Desmurget M, Sirigu A (2012) Conscious motor intention emerges in the inferior parietal lobule. Curr Opin Neurobiol 22:1004–1011

Dimitriadis SI, Laskaris NA, Micheloyannis S (2015) Transition dynamics of EEG-based network microstates during mental arithmetic and resting wakefulness reflects task-related modulations and developmental changes. Cogn Neurodyn 9:371–387

Dosenbach NUF et al (2010) Prediction of individual brain maturity using fMRI. Science 329:1358–1361

Eddy DR, Schiflett SG, Schlegel RE, Shehab RL (1998) Cognitive performance aboard the life and microgravity spacelab. Acta Astronaut 43:193–210

Epstein RA (2008) Parahippocampal and retrosplenial contributions to human spatial navigation. Trend Cogn Sci 12:388–396

Epstein RA, Parker WE, Feiler AM (2007) Where am I now? Distinct roles for parahippocampal and retrosplenial cortices in place recognition. J Neurosci 27:6141–6149

Fawcett T (2006) An introduction to ROC analysis. Pattern Recogn Lett 27:861–874

Garrity AG, Pearlson GD, McKiernan K, Lloyd D, Kiehl KA, Calhoun VD (2007) Aberrant "default mode" functional connectivity in schizophrenia. Am J Psychiatry 164:450–457

Grigoriev AI, Egorov AD (1992) General mechanisms of the effect of weightlessness on the human body. Adv Space Biol Med 2:1–42

Haber SN, Calzavara R (2009) The cortico-basal ganglia integrative network: the role of the thalamus. Brain Res Bull 78:69–74

Henderson JM, Larson CL, Zhu DC (2007) Cortical activation to indoor versus outdoor scenes: an fMRI study. Exp Brain Res 179:75–84

Henderson JM, Larson CL, Zhu DC (2008) Full scenes produce more activation than close-up scenes and scene-diagnostic objects in parahippocampal and retrosplenial cortex: an fMRI study. Brain Cogn 66:40–49

Hoffstaedter F et al (2014) The role of anterior midcingulate cortex in cognitive motor control. Hum Brain Mapp 35:2741–2753

Kawai Y, Doi M, Setogawa A, Shimoyama R, Ueda K, Asai Y (2003) Effects of microgravity on cerebral hemodynamics. Yonago Acta Med 46:1–8

Kosaki Y, Lin TCE, Horne MR, Pearce JM, Gilroy KE (2014) The role of the hippocampus in passive and active spatial learning. Hippocampus 24:1633–1652

Leung H, Gore JC, Goldman-Rakic PS (2002) Sustained mnemonic response in the human middle frontal gyrus during on-line storage of spatial memoranda. J Cogn Neurosci 14:659–671

Liao Y, Zhang J, Huang Z, Xi Y, Zhang Q, Zhu T, Liu X (2012) Altered baseline brain activity with 72 h of simulated microgravity—initial evidence from resting-state fMRI. PLoS One 7:e52558

Liao Y, Miao D, Huan Y, Yin H, Xi Y, Liu X (2013) Altered regional homogeneity with short-term simulated microgravity and its relationship with changed performance in mental transformation. PLoS One 8:e64931

Liao Y, Lei M, Huang H, Wang C, Duan J, Li H, Liu X (2015) The time course of altered brain activity during 7-day simulated microgravity. Front Behav Neurosci 9:124

Lockhart SN, Luck SJ, Geng J, Beckett L, Disbrow EA, Carmichael O, DeCarli C (2015) White matter hyperintensities among older adults are associated with futile increase in frontal activation and functional connectivity during spatial search. PLoS One 10:e0122445

Maguire E (2001) The retrosplenial contribution to human navigation: a review of lesion and neuroimaging findings. Scand J Psychol 42:225–238

Mallis MM, De Roshia C (2005) Circadian rhythms, sleep, and performance in space. Aviat Space Environ Med 76:B94–B107

Manzey D, Lorenz B, Heuer H, Sangals J (2000) Impairments of manual tracking performance during spaceflight: more converging evidence from a 20-day space mission. Ergonomics 43:589–609

Messerotti Benvenuti S, Bianchin M, Angrilli A (2011) Effects of simulated microgravity on brain plasticity: a startle reflex habituation study. Physiol Behav 104:503–506

Moore ST, Mac Dougall HG, Paloski WH (2010) Effects of head-down bed rest and artificial gravity on spatial orientation. Exp Brain Res 204:617–622

Owen AM, Milner B, Petrides M, Evans AC (1996) A specific role for the right parahippocampal gyrus in the retrieval of object-location: a positron emission tomography study. J Cogn Neurosci 8:588–602

Pavy-Le Traon A, Heer M, Narici MV, Rittweger J, Vernikos J (2007) From space to Earth: advances in human physiology from 20 years of bed rest studies (1986–2006). Eur J Appl Physiol 101:143–194

Pearce JM, Good MA, Jones PM, McGregor A (2004) Transfer of spatial behavior between different environments: implications for theories of spatial learning and for the role of the hippocampus in spatial learning. J Exp Psychol Anim Behav Process 30:135–147

Renier LA, Anurova I, De Volder AG, Carlson S, VanMeter J, Rauschecker JP (2010) Preserved functional specialization for spatial processing in the middle occipital gyrus of the early blind. Neuron 68:138–148

Roweis ST, Saul LK (2000) Nonlinear dimensionality reduction by locally linear embedding. Science 290:2323–2326

Seth A (2008) Causal networks in simulated neural systems. Cogn Neurodyn 2:49–64

Shirer WR, Ryali S, Rykhlevskaia E, Menon V, Greicius MD (2012) Decoding subject-driven cognitive states with whole-brain connectivity patterns. Cereb Cortex 22:158–165

Spiers HJ, Maguire EA (2006) Thoughts, behaviour, and brain dynamics during navigation in the real world. NeuroImage 31:1826–1840

Spreng RN, Mar RA, Kim AS (2009) The common neural basis of autobiographical memory, prospection, navigation, theory of mind, and the default mode: a quantitative meta-analysis. J Cogn Neurosci 21:489–510

Vaitl D, Gruppe H, Stark R, Pössel P (1996) Simulated micro-gravity and cortical inhibition: a study of the hemodynamic-brain interaction. Biol Psychol 42:87–103

Vann SD, Aggleton JP (2002) Extensive cytotoxic lesions of the rat retrosplenial cortex reveal consistent deficits on tasks that tax allocentric spatial memory. Behav Neurosci 116:85

Vann SD, Aggleton JP (2004) Testing the importance of the retrosplenial guidance system: effects of different sized retrosplenial cortex lesions on heading direction and spatial working memory. Behav Brain Res 155:97–108

Vann SD, Aggleton JP, Maguire EA (2009) What does the retrosplenial cortex do? Nat Rev Neurosci 10:792–802

Vapnik V (1995) The natures of statistical learning theory. Springer, New York

Wilmer A, de Lussanet MHE, Lappe M (2010) A method for the estimation of functional brain connectivity from time-series data. Cogn Neurodyn 4:133–149

Zeng L-L et al (2012) Identifying major depression using whole-brain functional connectivity: a multivariate pattern analysis. Brain 135:1498–1507

Zeng L-L et al (2014) Neurobiological basis of head motion in brain imaging. Proc Natl Acad Sci USA 111:6058–6062

Zhao X, Wang Y, Zhou R, Wang L, Tan C (2011) The influence on individual working memory during 15 days—6° head-down bed rest. Acta Astronaut 69:969–974

Zhou Y et al (2014) Disrupted resting-state functional architecture of the brain after 45-day simulated microgravity. Front Behav Neurosci 8:200